Study of the $K^- \to \pi^0 e^- \nu$ decay

I.V. Ajinenko, S.A. Akimenko, K.S. Belous, G.I. Britvich, I.G. Britvich, K.V. Datsko,
A.P. Filin, A.V. Inyakin, A.S. Konstantinov, V.F. Konstantinov, I.Y. Korolkov,
V.A. Khmelnikov, V.M. Leontiev, V.P. Novikov, V.F. Obraztsov, V.A. Polyakov,
V.I. Romanovsky, V.M. Ronjin, V.I. Shelikhov, N.E. Smirnov, A.A. Sokolov,
O.G. Tchikilev, V.A. Uvarov, O.P. Yushchenko

Institute for High Energy Physics, Protvino, Russia

V.N. Bolotov, S.V. Laptev, A.R. Pastsjak, A.Yu. Polyarush, R.Kh. Sirodeev

Institute for Nuclear Research, Moscow, Russia

Abstract

The decay $K^- \to \pi^0 e \nu$ has been studied using in-flight decays detected with the "ISTRA+" spectrometer operating in the 25-GeV negative secondary beam of the U-70 PS. About 550K events were collected for the analysis. The λ_+ parameter of the vector form-factor has been measured: $\lambda_+ = 0.0286 \pm 0.0008(\text{stat}) \pm 0.0006(\text{syst})$. The limits on the possible tensor and scalar couplings have been obtained: $f_T/f_+(0) = 0.021^{+0.064}_{-0.075}(\text{stat}) \pm 0.026(\text{syst})$; $f_S/f_+(0) = 0.002^{+0.020}_{-0.022}(\text{stat}) \pm 0.003(\text{syst})$.

© 2003 Published by Elsevier B.V. Open access under CC BY license.

1. Introduction

The decay $K \to e\nu\pi^0 (K_{e3})$ is known to be a very promising one to search for an admixture of scalar (S) or tensor (T) contributions to the Standard Model (SM) V-A amplitude. This decay has been extensively studied over recent years in different experiments with the charged and neutral kaons. Some published results indicate the anomalous S and T signals [1,2].

On the other hand, a recent KEK experiment [3,4] with a stopped K^+ beam and our preliminary studies [5] do not observe any visible contributions of tensor and scalar interactions. Another goal of our study is a precise measurement of the V-A $f_+(t)$ form-factor of the K_{e3} decay which is interesting in view of new calculations in the chiral perturbation theory (ChPT) up to the order p^6 [6].
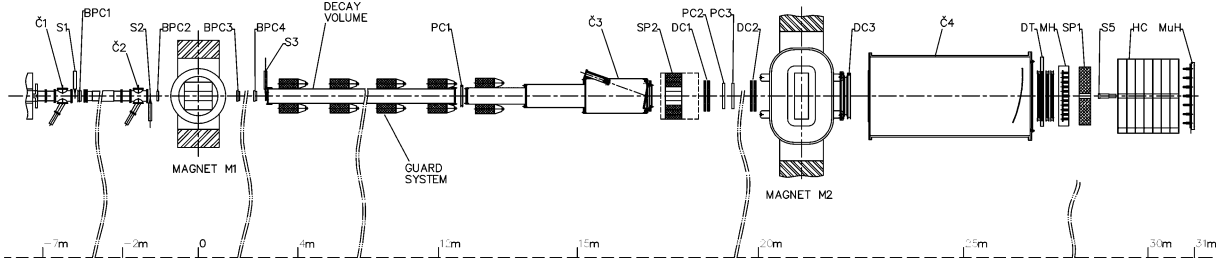
Fig. 1. Elevation view of the "ISTRA+" detector.

We present a new study of the K_{e3}^- decay based on the statistics of about 550K events. This analysis is an update of our preliminary results [5].

2. Experimental setup

The experiment has been performed at the IHEP 70 GeV proton synchrotron U-70. The experimental setup "ISTRA+" (Fig. 1) was described in some details in our paper [5].

The setup is located in a negative unseparated secondary beam. The beam momentum is ~ 25 GeV with $\Delta p/p \sim 1.5\%$. The admixture of K^- in the beam is $\sim 3\%$. The beam intensity is $\sim 3 \times 10^6$ per 1.9 s of the U-70 spill. The beam particles are deflected by the beam magnet M1 and are measured by BPC_1–BPC_4 proportional chambers with 1 mm wire spacing. The kaon identification is performed by $\check{C}_0$–$\check{C}_2$ threshold $\check{C}$-counters.

The 9 meter long vacuumed decay volume is surrounded by 8 lead-glass rings LG_1–LG_8 which are used as the veto system for low energy photons. The photons radiated at large angles are detected by the lead-glass calorimeter SP_2.

The decay products are deflected by the spectrometer magnet M2 with a field integral of 1 Tm. The track measurement is performed by 2-mm-step proportional chambers (PC_1–PC_3), 1-cm-cell drift chambers (DC_1–DC_3), and by 2-cm-diameter drift tubes (DT_1–DT_4). Wide aperture threshold Čerenkov counters ($\check{C}_3$ and $\check{C}_4$) are filled with helium and are not used in these measurements.

The photons are measured by the lead-glass calorimeter SP_1 which consists of 576 counters. The

counter transverse size is 5.2×5.2 cm and the length is about 15 X_0.

The scintillator-iron sampling hadron calorimeter HC is subdivided into 7 longitudinal sections $7{\times}7$ cells each. The $11{\times}11$ cell scintillating hodoscope is used for the improvement of the time resolution of the tracking system. MuH is a $7{\times}7$ cell scintillating muon hodoscope.

The trigger is provided by S_1–S_5 scintillation counters, $\check{C}_0$–$\check{C}_2$ Cerenkov counters, and the analog sum of amplitudes from last dinodes of the SP_1:

$$T = S_1 \cdot S_2 \cdot S_3 \cdot \bar{S}_4 \cdot \check{C}_0 \cdot \bar{\check{C}}_1 \cdot \bar{\check{C}}_2 \cdot \bar{S}_5 \cdot \Sigma(SP_1),$$

where S_4 is the scintillator counter with a hole to suppress the beam halo, S_5 is the counter located downstream the setup at the beam focus, $\Sigma(SP_1)$ requires that the analog sum of amplitudes from the SP_1 be larger than ~ 700 MeV—a MIP signal. The last requirement serves to suppress the dominating $K \to \mu\nu$ decay.

3. Events selection

During runs in Spring (run1) and Winter (run2) 2001, 363M and 332M events were logged on tapes. This statistics is supported by about 260M MC events generated with Geant3 [7] Monte Carlo program. The MC generation includes a realistic description of the setup with decay volume entrance windows, tracking chambers windows, chambers gas mixtures, sense wires and cathode structures, Čerenkov counters mirrors and gas, the shower generation in EM calorimeters, etc.

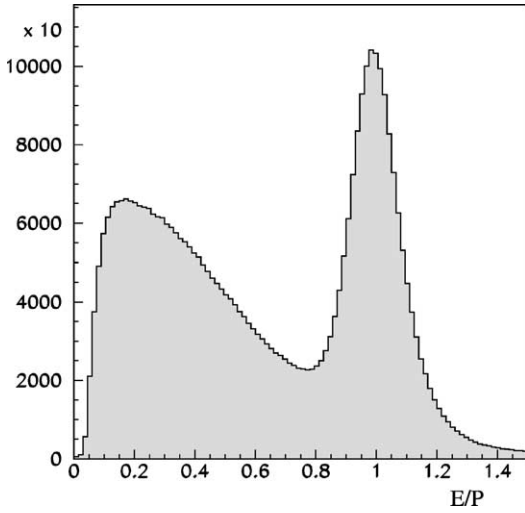The data processing starts with the beam particle reconstruction in BPC_1–BPC_4. Then secondary tracks

Fig. 2. The ratio of the energy of the associated ECAL cluster to the momentum of the charged track.

Fig. 4. The beam kaon momentum after 2C K_{e3} fit. The points with errors are the run2 data and the histogram is MC.
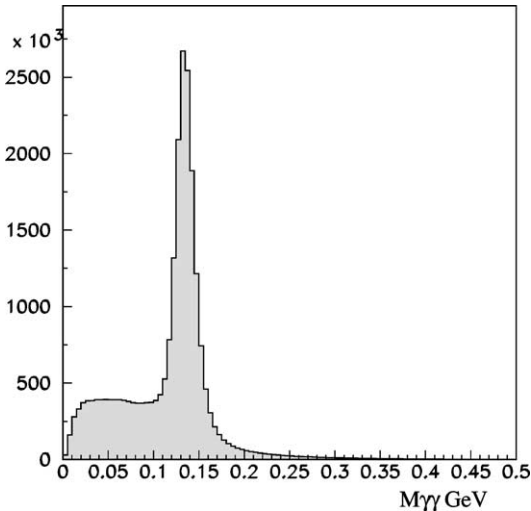

Fig. 3. The $\gamma\gamma$-mass spectrum for the events with the identified electron and two extra showers.

are looked for in the decay tracking system and events with one good negatively charged track are selected. The decay vertex is reconstructed by means of the unconstrained vertex fit of the beam and decay tracks.

A clustering procedure is used to find showers in the SP_1 calorimeter, and the two-dimensional pattern of the shower is fitted with the MC-generated patterns to reconstruct its energy and position.
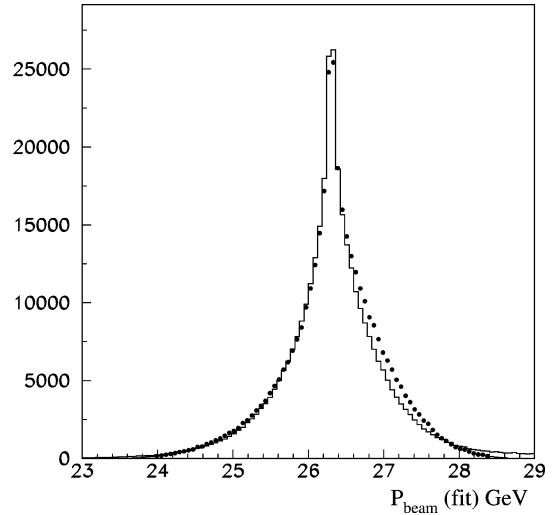
The matching of the charged track and a shower in SP_1 is done on the basis of the distance r between the track extrapolation to the calorimeter and the shower coordinates ($r \leqslant 3$cm). The electron identification is done using the ratio of the shower energy (E) to the momentum of the associated track (p). The E/p distribution is shown in Fig. 2. The particles with $0.8 < E/p < 1.3$ are accepted as electrons.

The events with one charged track identified as electron and two additional showers in the ECAL are selected for further processing. The $\gamma\gamma$-mass spectrum is shown in Fig. 3. The π^0 peak is situated at $M_{\pi0} = 134.8$ MeV with a resolution of 8.6 MeV.

The selected events are required to pass 2C $K \to e\nu\pi^0$ fit. To minimize effects of a beam associated background and systematics the cut on the difference between the fitted P_K value and the mean beam energy (25.2 GeV for the first run and 26.3 GeV for the second) is applied: $|P_K - \bar{P}_{\text{beam}}| < 1$ GeV (see Fig. 4). The missing energy $E_\nu = E_K - E_e - E_{\pi^0}$ at this stage of the selection is shown in Fig. 5 for run2 data.

The peak at low E_ν corresponds to the remaining $K^- \to \pi^-\pi^0$ background. The cut $E_\nu > 0.3$ GeV is applied to suppress this background. The requirement that the 5C $K \to \pi^-\pi^0$ fit should fail is applied for further background suppression.

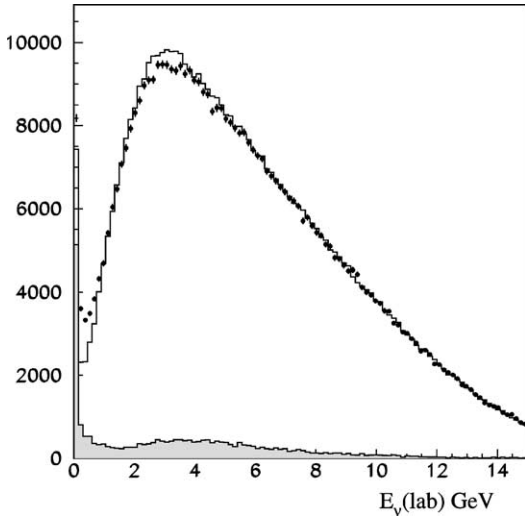The surviving background is estimated to be less than 1.5%.

Fig. 5. The E_ν energy compared with MC. The points are data, the dark histogram is the background contamination.

Fig. 6. Dalitz plot for the selected $K \to e\nu\pi^0$ events. Run2 data.

4. Analysis

Performing the procedure described in the previous section, 112K and 440K events are selected in run1 and run2 data. The difference in the event output is explained by the higher SP_1 analog sum threshold in the second run. The distribution of the events over the Dalitz plot for the run2 is shown in Fig. 6. The variables $y = 2E_e/M_K$ and $z = 2E_\pi/M_K$, where E_e and E_π are the energies of the electron and π^0 in the kaon rest frame, are used. The analysis of the MC-generated background shows that the background events are concentrated at the peripheral part of the plot.

The most general Lorentz-invariant form of the matrix element for the $K^- \to l^- \nu \pi^0$ decay is [8]:

$$M = \frac{G_F V_{us}}{2} \bar{u}(p_\nu)(1 + \gamma^5)$$
$$\times \bigg[2m_K f_S$$
$$- \big[(P_K + P_\pi)_\alpha f_+ + (P_K - P_\pi)_\alpha f_- \big] \gamma^\alpha$$
$$+ i \frac{2 f_T}{m_K} \sigma_{\alpha\beta} P_K^\alpha P_\pi^\beta \bigg] v(p_l). \quad (1)$$

It consists of scalar, vector, and tensor terms. The $f_\pm$ form-factors are the functions of $t = (P_K - P_\pi)^2$. In the Standard Model (SM), the W-boso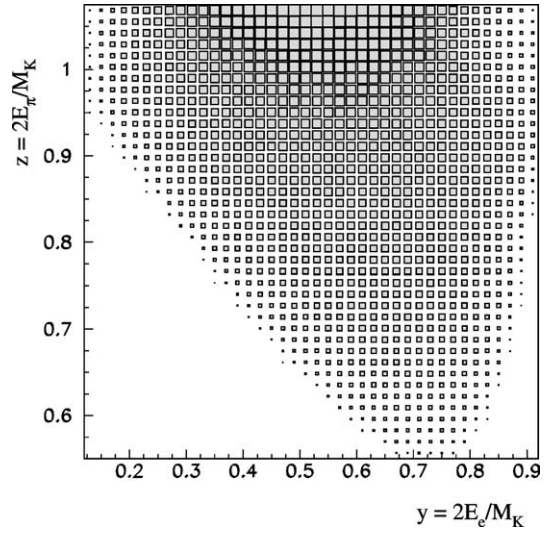n exchange leads to the pure vector term. The scalar and/or tensor terms which are "induced" by EW radiative corrections are negligibly small, i.e., nonzero scalar or tensor form-factors would indicate the physics beyond the SM.

The term in the vector part, proportional to f_-, is reduced (using the Dirac equation) to the scalar form-factor. In the same way, the tensor term is reduced to a mixture of the scalar and vector form-factors. The redefined vector (V) and scalar (S) terms, and the corresponding Dalitz plot density in the kaon rest frame ($\rho(E_\pi, E_l)$) are [9]:

$$\rho(E_\pi, E_l) \sim A|V|^2 + B \operatorname{Re}(V^* S) + C|S|^2,$$
$$V = f_+ + (m_l/m_K) f_T,$$
$$S = f_S + (m_l/2m_K) f_-$$
$$+ \left(1 + \frac{m_l^2}{2m_K^2} - \frac{2E_l}{m_K} - \frac{E_\pi}{m_K} \right) f_T,$$
$$A = m_K (2E_l E_\nu - m_K \Delta E_\pi) - m_l^2 \left(E_\nu - \frac{1}{4} \Delta E_\pi \right),$$
$$B = m_l m_K (2E_\nu - \Delta E_\pi),$$
$$E_\nu = m_K - E_l - E_\pi,$$
$$C = m_K^2 \Delta E_\pi, \qquad \Delta E_\pi = E_\pi^{\max} - E_\pi,$$
$$E_\pi^{\max} = \frac{m_K^2 - m_l^2 + m_\pi^2}{2m_K}. \quad (2)$$

The terms proportional to m_l and m_l^2 can be neglected in the case of the K_{e3} decay.

Then, assuming the linear dependence of the f_+ on t: $f_+(t) = f_+(0)(1 + \lambda_+ t/m_\pi^2)$ and real constants f_S, f_T, we get

$$\rho(E_\pi, E_l)$$

$$\sim m_K(2E_l E_\nu - m_K \Delta E_\pi)(1 + \lambda_+ t/m_\pi^2)^2$$

$$+ m_K^2 \Delta E_\pi \left(\frac{f_S}{f_+(0)} \right.$$

$$\left. + \left(1 - \frac{2E_l}{m_K} - \frac{E_\pi}{m_K} \right) \frac{f_T}{f_+(0)} \right)^2 .$$

$$(3)$$

The procedure of the extraction of the parameters λ_+, f_S, f_T starts with the subdivision of the Dalitz plot region $y = 0.12$–0.92; $z = 0.55$–1.075 into 40×40 cells.

The number of events in a cell (i, j) of the Dalitz plot, in the case of the simultaneous extraction of, for example, λ_+ and $f_S/f_+(0)$, is fitted by the function:

$$W^{\text{MC}}(i, j) \sim W_1(i, j) + W_2(i, j)\lambda_+ + W_3(i, j)\lambda_+^2$$

$$+ W_4(i, j) \left(\frac{f_S}{f_+(0)} \right)^2 . \qquad (4)$$

Here W_l are MC-generated functions which are built up as follows: the MC events are generated with the constant density over the Dalitz plot and reconstructed with the same program as for the real events. Each event carries the weight w determined by the corresponding term in the expression (3), calculated using the MC-generated "true" values for y and z. The radiative corrections according to [10] are taken into account. Then, W_l are calculated by summing up the weights of the reconstructed events in the corresponding Dalitz plot cell. This procedure allows one to avoid the systematic errors due to the "migration" of the

events over the Dalitz plot due to the finite experimental resolution.

The parameters of the amplitude of the decay are extracted by minimizing the extended log-likelihood function:

$$\mathcal{L} = \sum_{i,j} \left\{ \left(A W_{i,j}^{\text{MC}} + N_{ij}^{\text{bg}} - N_{i,j}^{\text{rd}} \right) \right.$$

$$\left. + N_{i,j}^{\text{rd}} \ln \frac{N_{i,j}^{\text{rd}}}{A W_{i,j}^{\text{MC}} + N_{ij}^{\text{bg}}} \right\}, \qquad (5)$$

where the sum runs over all populated cells of the Dalitz plot. Here A is the data/MC normalization parameter, N_{ij}^{rd}—number of real data events in the (i, j)-cell, and N_{ij}^{bg}—the MC estimated background. The background normalization is determined by the ratio of the real and generated $K^- \to \pi^- \pi^0$ events. The minimization is performed by means of the "MINUIT" program [11].

5. Results

The results of the fit are summarized in Table 1.

The combination of two runs is done by the simultaneous fit. The first line corresponds to the pure V-A SM fit. In the second line the tensor and, in the third, the scalar terms are added into the fit.

The final errors are calculated by the "MINOS" procedure of the "MINUIT" program [11]. The errors are estimated at the $2\Delta\mathcal{L}$ level of 2.3 that corresponds to the coverage probability of 68.27% for joint estimation of 2 parameters [13].

To illustrate the quality of the fit, Fig. 7 shows the ratio of the real data minus MC-predicted background $(N^{\text{rd}} - N^{\text{bg}})$ over W_{MC} versus $t/m_{\pi^0}^2$, calculated using expression (4), with $\lambda_+ = 0.0286$ and $f_T = f_S = 0$.

Table 1
Results of the fit

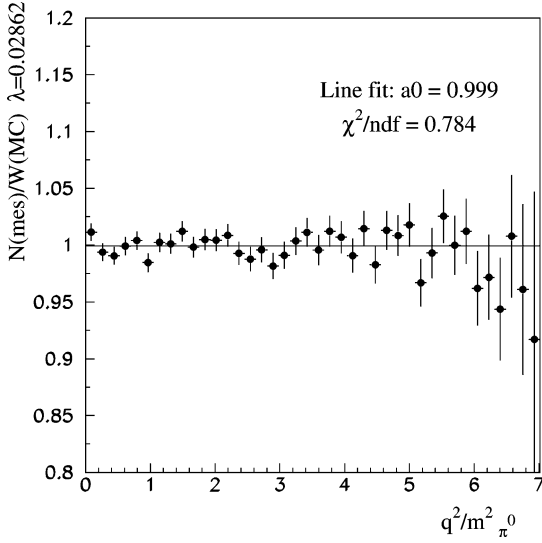|	run1	run2	run1 + run2
λ_+	0.0291 ± 0.0018	0.0285 ± 0.0009	0.0286 ± 0.0008
$f_T/f_+(0)$	$0.018^{+0.087}_{-0.099}$	$0.024^{+0.081}_{-0.107}$	$0.021^{+0.064}_{-0.075}$
$f_S/f_+(0)$	$0.003^{+0.024}_{-0.029}$	$0.002^{+0.019}_{-0.032}$	$0.002^{+0.020}_{-0.022}$
χ^2/ndf	1.13	1.14	1.14
N_{bins}	1120	1119	2239

Fig. 7. The ratio $(N^{\mathrm{rd}} - N^{\mathrm{bg}})/W_{\mathrm{MC}}$ (see text) for the run1 + run2 data.

Different sources of systematics are investigated:

- The Dalitz plot binning:
  $\Delta\lambda_+ = \pm 0.00006$; $\Delta f_T = \pm 0.003$; $\Delta f_S = \pm 0.0006$. This kind of systematics is very small in our case because of the fitting method (see expression (4)).
- Selection cuts variation:
  (1) The 5C $K \to \pi^-\pi^0$ fit probability cut:
  $\Delta\lambda_+ = \pm 0.00041$; $\Delta f_T = \pm 0.0144$; $\Delta f_S = \pm 0.0018$.
  (2) The 2C $K \to e\nu\pi^0$ fit probability cut:
  $\Delta\lambda_+ = \pm 0.00025$; $\Delta f_T = \pm 0.008$; $\Delta f_S = \pm 0.0012$.
  (3) The missing energy (E_ν) cut:
  $\Delta\lambda_+ = \pm 0.00015$; $\Delta f_T = \pm 0.0081$; $\Delta f_S = \pm 0.0008$.
  (4) The $|P_K - \bar{P}_{\mathrm{beam}}|$ cut:
  $\Delta\lambda_+ = \pm 0.00026$; $\Delta f_T = \pm 0.0104$; $\Delta f_S = \pm 0.0018$.
  (5) The E/p electron selection cut:
  $\Delta\lambda_+ = \pm 0.00014$; $\Delta f_T = \pm 0.010$; $\Delta f_S = \pm 0.0008$.
- The signal MC variation: $\Delta\lambda_+ = \pm 0.00005$; $\Delta f_T = \pm 0.001$; $\Delta f_S = \pm 0.0001$.
- The background MC variation: $\Delta\lambda_+ = \pm 0.00015$; $\Delta f_T = \pm 0.011$; $\Delta f_S = \pm 0.0003$.

From that, the total systematics is: $\Delta\lambda_+ = \pm 0.0006$; $\Delta f_T = \pm 0.026$; $\Delta f_S = \pm 0.003$.

The comparison of our results with the most recent $K^\pm$ data [1,4] shows very good agreement in the λ_+ parameter. We do not observe any visible contributions of scalar and tensor terms in the amplitude, in agreement with the conclusions of [4,5].

Some difference (2σ) with the ChPT O(p^4) calculations for λ_+: $\lambda_+ = 0.031$ [12], is observed.

In addition, a possible contribution of the quadratic term $\lambda''_+ t^2/m_\pi^4$ into the f_+ form-factor is searched for. The value of $\lambda''_+ = -0.00042^{+0.0011}_{-0.0015}$ is obtained with the fixed $\lambda_+ = 0.0286$. If λ_+ is allowed to vary, its value is shifted to $\lambda_+ = 0.02867 \pm 0.0020$ and the quadratic coefficient becomes $\lambda''_+ = -0.002^{+0.0031}_{-0.0066}$. We conclude that a possible quadratic contribution into the vector form-factor is compatible with zero in both cases.

6. Summary and conclusions

The K^-_{e3} decay has been studied using in-flight decays of 25 GeV K^-, detected by the "ISTRA+" magnetic spectrometer. Due to the high statistics, adequate resolution of the detector, and good sensitivity over all the Dalitz plot space, the errors in the fitted parameters are significantly reduced as compared with the previous measurements.

The λ_+ parameter of the vector form-factor is measured to be

$$\lambda_+ = 0.0286 \pm 0.0008(\mathrm{stat}) \pm 0.0006(\mathrm{syst}).$$

The limit on the quadratic nonlinearity for $f_+(t)$ is obtained

$$\lambda''_+ = -0.00042^{+0.0011}_{-0.0015}(\mathrm{stat}).$$

The limits on the possible tensor and scalar couplings are derived:

$$f_T/f_+(0) = 0.021^{+0.064}_{-0.075}(\mathrm{stat}) \pm 0.026(\mathrm{syst}),$$
$$f_S/f_+(0) = 0.002^{+0.020}_{-0.022}(\mathrm{stat}) \pm 0.003(\mathrm{syst}).$$

References

[1] S.A. Akimenko, et al., Phys. Lett. B 259 (1991) 225.
[2] R.J. Tesarek, hep-ex/9903069.
[3] S. Shimizu, et al., Phys. Lett. B 495 (2000) 33.
[4] A.S. Levchenko, et al., Yad. Fiz. 65 (2002) 2294, hep-ex/0111048.
[5] I.V. Ajinenko, et al., Yad. Fiz. 65 (2002) 2125.
[6] J. Bijnens, hep-ph/0303103.
[7] R. Brun, et al., CERN-DD/EE/84-1.
[8] H. Steiner, et al., Phys. Lett. B 36 (1971) 521.
[9] M.V. Chizhov, hep-ph/9511287.
[10] E.S. Ginsberg, Phys. Rev. 162 (1967) 1570.
[11] F. James, M. Roos, CERN D506, 1989.
[12] J. Gasser, H. Leutwyler, Nucl. Phys. B 250 (1985) 517.
[13] Particle Data Group, Review of Particle Physics, Phys. Rev. D 66 (2002) 1.